TECHNICAL ARTICLE

Analysis of preferential orientation in zirconium samples deformed by uniaxial tension using neutron and X-ray diffraction

M. Kučeráková,[1,a] S. Vratislav,[1] L. Kalvoda,[1] and Z. Trojanová[2]
[1]*Czech Technical University in Prague, Czech Republic*
[2]*Faculty of Mathematics and Physics, Czech Republic*

(Received 2 October 2014; accepted 10 November 2014)

Two series of zirconium samples were investigated by neutron and X-ray diffraction. First series of the samples was deformed at room temperature (RT), whereas the second series was deformed at 300 °C. Both series were deformed on uniaxial tensile machine INSTRON 5882 from strain 0 to 30% (strain step was 5%). The neutronographic texture measurements were performed on the KSN-2 neutron diffractometer located at the research reactor LVR-15 in the Nuclear Research Institute, plc. Rez, Czech Republic. The X-ray measurements were performed at the theta/theta X'Pert PRO diffractometer with the Cr X-ray tube. Observed data were processed by the software packages GSAS and X'Pert Texture. Preferential orientation of the $(10\bar{1}0)$ and $(11\bar{2}0)$ plane poles is found to be parallel to the rolling direction for both tested deformation series. Poles of the $(10\bar{1}2)$ and $(10\bar{1}3)$ planes tend to be parallel to the normal direction (Tables II and III). Orientation of the basal poles is tilted by 45° from the normal direction toward the transverse direction. Sharpness of the resulting texture increases with extends of the applied deformation as well as with rise of the tensile test temperature from the RT level to 300 °C. © *2015 International Centre for Diffraction Data.*
[doi:10.1017/S0885715614001316]

Key words: preferred orientation, zirconium, uniaxial strain, neutron diffraction, X-ray diffraction

I. INTRODUCTION

Zirconium is a metal with below-normal *c*/*a* ratio (*c*/*a* <1633). Zirconium has very low absorption cross-section for thermal neutrons, high hardness, ductility, and corrosion resistance. Therefore, zirconium and zirconium-rich alloys are used in the nuclear industry, specifically for the fuel element cladding tubes of light water reactors (Murty, 1989). Coated tubes form a barrier against the escape of fission products into the coolant, contributing at the same time to the geometrical stability of the reactor active zone. For the crucial importance for nuclear reactor safety, an extraordinary attention is paid to the properties and behavior of zirconium under extreme conditions.

To better understand such behavior and further improve operating characteristics of the fuel, it is also very important to examine in detail the dependence of the zirconium mechanical properties on its structure and texture. The present paper aims to contribute to the mentioned issues by revealing the texture changes caused in α-zirconium by application of uniaxial tension performed under several different conditions.

In our work, the texture of two series of zirconium samples is investigated by means of neutron and X-ray diffraction. The first set of samples was deformed on uniaxial tensile machine INSTRON 5882 at room temperature (RT), whereas an elevated temperature (300 °C) was applied during the second set deformation. Both the series of samples were deformed in the step-like manner (strain step 5%) up to the final strain 30%.

Experimental pole figures are used, together with values of inverse pole figures calculated by Mueller formula (Horta *et al.*, 1969), to analyze the preferential orientation of grains.

A majority of zirconium texture analyses deals, in the first order, with the basal pole distribution being of a key importance for the resulting material properties. On the other hand, distribution of prismatic or pyramidal plane poles can serve as a strong indicator for the degree of annealing and, moreover, is of significant importance for a more detail quantitative texture analysis performed by means of the orientation distribution function (ODF) of grains (Tenckhoff, 2005).

Plastic deformation in α-zirconium is realized by slip and twinning mechanisms. The most frequent slip occurs on the $\{10\bar{1}0\}$ first-order prism planes along the $\langle 12\bar{3}0\rangle$ direction. The same direction is preferred in the case of slip on the basal planes. In regions of a high-stress concentration, the $\{10\bar{1}1\}$ slip is observed. Activation of slip with the $\langle c\rangle$ component was also noticed on the first- and second-order pyramidal planes $\{10\bar{1}1\}$ and $\{11\bar{2}1\}$ along the $\langle c+a\rangle$ direction (Tenckhoff, 2005). Most common twinning modes are $\{10\bar{1}2\}$ $\langle\bar{1}011\rangle$ tensile twins and $\{11\bar{2}2\}\langle\bar{1}\bar{1}23\rangle$ compressive twins at RT and $\{10\bar{1}1\}\langle 10\bar{1}2\rangle$ twins at the elevated temperatures (Tenckhoff, 2005).

II. SAMPLES

The initial α-zirconium plate was forged, hot rolled to the thickness 3.3 mm and annealed at 664 °C for several hours. Shape, dimensions, and coordination system of the tensile specimens prepared from the treated plate are shown in Figure 1 (here ND, TD, and RD stand for the normal, transverse, and rolling directions, respectively). The purity of the

[a]Author to whom correspondence should be addressed. Electronic mail: monika.kucerakova@fjfi.cvut.cz

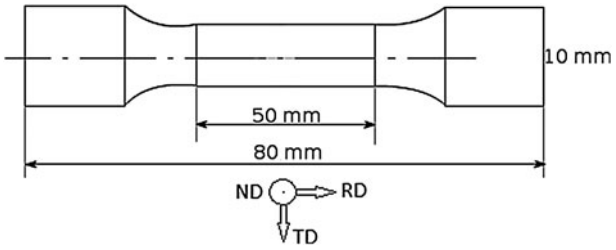

Figure 1. Shape and dimensions of measured zirconium samples.

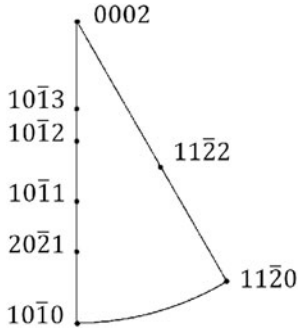

Figure 2. Location of the reflection plane poles on the stereographic projection of the symmetrically non-equivalent spherical triangle of α-zirconium.

zirconium material was checked by mass spectroscopy and the vacuum extraction method. The main impurities are indicated in Table I.

III. DIFFRACTION EXPERIMENTS

The neutronographic texture measurements were performed on the KSN-2 neutron diffractometer situated at the horizontal channel of the research reactor LVR-15 located in the Nuclear Research Institute, plc. Rez, Czech Republic. The monochromatic neutrons having wavelength 0.1362 nm were used. The single-crystal Cu(200) was used as monochromator. The KSN-2 diffraction device offers good intensity and the best resolution value of $\Delta d/d = 0.007$ in the region $d \sim 1.0 \div 0.1$ nm (d is interplanar spacing). The samples were mounted in reflection geometry with its normal parallel to the direction of interest – usually RD, TD, or ND – and the reflected intensities were measured depending on the Bragg angle. All the obtained neutronographic patterns were corrected for the non-linear background and then evaluated using the Rietveld method implemented in the software package GSAS (Larson *et al*., 1997). The resulting peak intensities were normalized to the intensities of a standard sample (sample with grains randomly oriented) using the Mueller formula and the relative pole densities of the selected crystallographic planes p_{hkil} along the principal directions ND, RD, and TD were obtained. The latter reflect the relative level of the preference of the grains being oriented with the particular crystallographic direction along the corresponding direction of the specimen under test. In untextured sample with random orientation of grains, $p_{hkil} = 1$. Value $p_{hkil} > 1$ along a certain specimen direction says that, within the tested sample volume, more crystalline grains are oriented by the examined plane {*hkil* poles parallel to the selected specimen direction than it is the case in the untextured specimen. The method and its application on characterization of zirconium textures is in more details described elsewhere (Vetvicka, 2014).

Figure 2 shows the positions of crystallographic poles within the inverse pole figure of zirconium.

The X-ray texture measurements were performed at theta/theta X'Pert PRO diffractometer with Cr X-ray tube. The range of the sample inclinations was from 0° to 80°. Full pole figures for planes (0002) and $(10\bar{1}0)$ were calculated from the ODF determined using the measured incomplete pole figures (the limiting polar angle being 70°). Software package X'Pert Texture, PANalytical was used to perform the calculations.

TABLE I. Amount of impurities in the measured zirconium samples.

Hf (at%)	Ca (at%)	Mg (at%)	O (at%)	H (at%)
0.41	0.044	0.096	0.055	0.0011

IV. RESULTS

Pole densities p_{hkil} calculated by the Mueller formula are summarized in Table II (RT) and Table III (300 °C).

Measured pole figures for planes (0002) and $(10\bar{1}0)$ for samples deformed at 5, 15, and 30% at RT and 300 °C are shown in Figure 3.

V. DISCUSSION

The orientation of basal poles is found to be tilted from ND toward TD by ±45° for both deformation conditions (Figure 3). Such orientation was already observed (Santisteban *et al.*, 2012) and interpreted as evidence of $\{11\bar{2}2\}\langle\bar{1}\bar{1}23\rangle$ compressive twinning mode around 60°. The intensity ratios

TABLE II. Calculated p_{hkil} values of the chosen crystallographic planes (cf. Figure 2) and the principal specimen directions obtained for the samples deformed at RT.

	p^{ND}_{0002}	p^{TD}_{0002}	$p^{ND}_{10\bar{1}2}$	$p^{ND}_{10\bar{1}3}$	$p^{RD}_{10\bar{1}0}$	$p^{RD}_{11\bar{2}0}$
0%	2.82	1.27	1.74	1.65	1.43	1.72
5%	2.67	1.73	1.58	1.41	1.51	1.45
10%	2.60	1.76	1.62	1.55	2.19	1.42
15%	2.77	2.01	1.36	1.34	2.49	1.45
20%	2.91	2.12	1.20	1.20	1.58	0.72
25%	2.85	2.27	1.48	1.52	2.34	0.83
30%	2.77	3.30	1.38	1.42	2.67	0.87

TABLE III. Calculated p_{hkil} values of the chosen crystallographic planes (cf. Figure 2) and the principal specimen directions obtained for the samples deformed at 300 °C.

	p^{ND}_{0002}	p^{TD}_{0002}	$p^{ND}_{10\bar{1}2}$	$p^{ND}_{10\bar{1}3}$	$p^{RD}_{10\bar{1}0}$	$p^{RD}_{11\bar{2}0}$
0%	2.82	1.27	1.74	1.65	1.43	1.72
5%	2.35	1.66	1.83	1.65	2.93	2.74
10%	2.92	1.58	1.50	1.42	3.42	2.16
15%	2.87	2.08	1.60	1.38	3.77	1.95
20%	2.95	2.03	1.42	1.27	3.78	1.71
25%	3.02	2.41	1.37	1.31	4.66	1.38
30%	3.56	1.50	1.44	1.27	4.39	1.32

https://doi.org/10.1017/S0885715614001316 Published online by Cambridge University Press

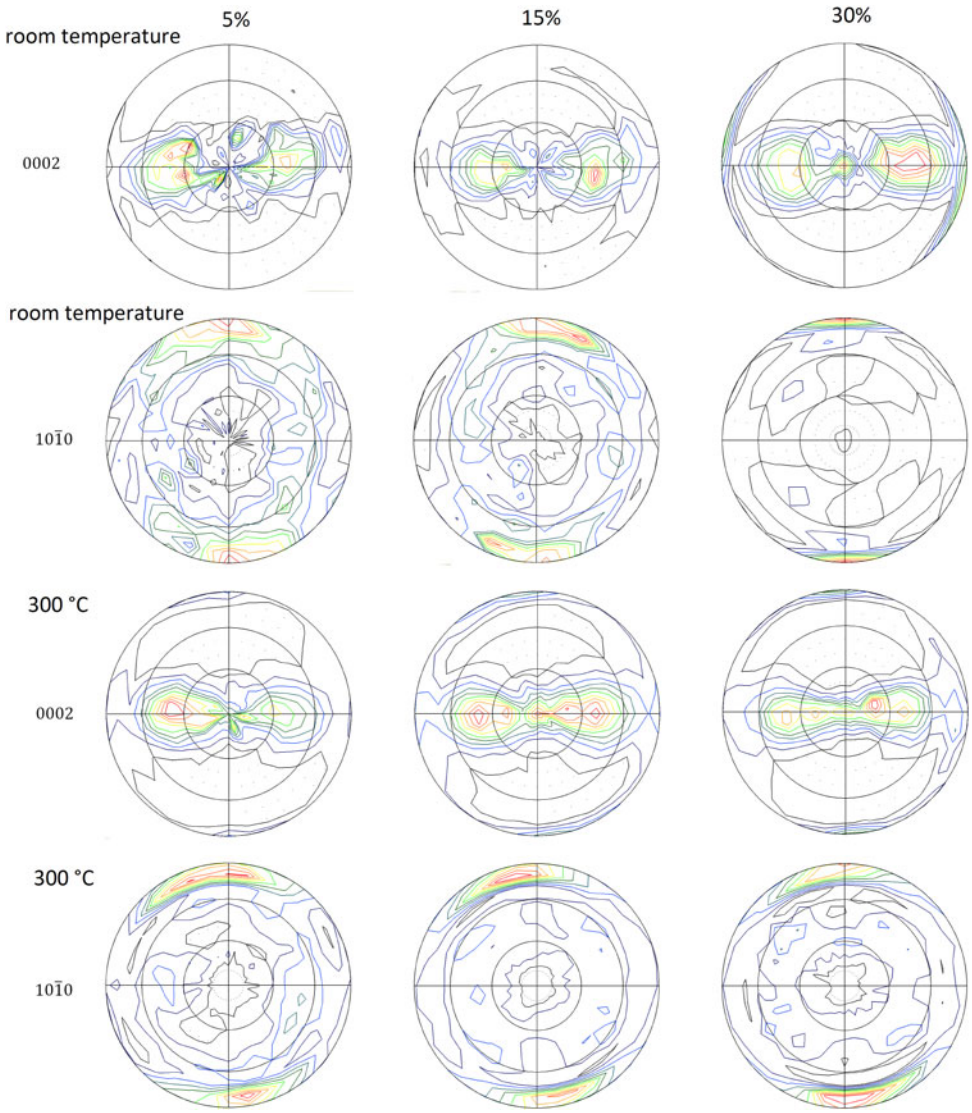

Figure 3. (Colour online) Pole figures of planes (0002) and (10$\bar{1}$0) observed for the samples deformed at 5, 15, and 30% at RT and 300 °C, respectively.

p_{hkil} (Tables II and III) are compatible with latter result. The values p^{ND}_{0002} and p^{TD}_{0002} are significantly higher than 1 and the value of p^{TD}_{0002} is markedly increasing with the deformation ratio, especially for the samples deformed at RT, what indicates a gradual tilt of the basal poles toward TD. The value of pole density p^{ND}_{0002} does not significantly change during the deformation at RT (Table II). On the other hand, p^{ND}_{0002} grows remarkably (from 2.82 to 3.56) during the deformation at 300 °C (Table III).

Santisteban *et al.* (2012) observed that part of the {0002} poles was also oriented along the tensile direction (RD) for samples deformed at RT as well as at 300 °C. Such rotation coheres with the $\{10\bar{1}2\}\langle 10\bar{1}1\rangle$ tensile twinning mode (Allen *et al.*, 2009). In our case, such orientation is only found in X-ray pole figures obtained on the sample deformed at 300 °C. No evidence for such texture component is indicated by neutron diffraction giving values p^{RD}_{0002} around 0.01 and 0.1 for samples deformed at RT and 300 °C, respectively.

From the calculated values $p^{\mathrm{RD}}_{10\bar{1}0}$ (Tables II and III) it follows that $(10\bar{1}0)$ plane poles orient to be parallel to RD for both deformation conditions. The same situation is observed in case of $(11\bar{2}0)$ planes.

The $(10\bar{1}2)$ and $(10\bar{1}3)$ plane poles prefer to be collinear with ND (Tables II and III).

VI. CONCLUSIONS

The above-mentioned texture changes observed on the α-zirconium samples subjected to tensile test performed under different thermal conditions can be summarized as follows:

- The rotation of {0002} poles from the normal direction toward the transverse direction is remarkably preferred for all the measured samples and is not affected by change of the tensile test conditions.
- From the X-ray texture measurements it can be seen that the $\{10\bar{1}2\}\langle 10\bar{1}1\rangle$ tensile twinning mode is taking place for the deformation performed at 300 °C only.
- The temperature increase of the tensile test from the RT to 300 °C results in increase of the overall texture sharpness.
- Bulk texture provided by neutron diffraction generally corresponds with the texture obtained by the X-ray diffraction.
- Overall level of the resulting texture increases the deformation progress.

https://doi.org/10.1017/S0885715614001316 Published online by Cambridge University Press

ACKNOWLEDGEMENTS

This work was supported by the Grant Agency of the Czech Technical University in Prague (grant no. SGS13/219/OHK4/3T/14) and the Czech Science Foundation (grant no. GACR 14-36566G).

Allen, V. M., Quinta da Fonseca, J., Preuss, M., Robson, J. D., Daymond, M. R., and Comstock, R. J. (**2009**). "Determination and interpretation of texture evolution during deformation of a zirconium alloy," J. ASTM Int., **5**, 377–390.

Horta, R. M. S. B., Roberts, W. T., and Wilson, D. V. (**1969**). Texture representation by inverse pole figures. In *Transactions of the Metallurgical Society of AIME*, **245** (12), 2525.

Larson, A. C. and Von Dreele, R. B. (**1997**). *General Structure Analysis System (GSAS) (Report LAUR 86-748)*. Los Alamos, New Mexico: Los Alamos National Laboratory.

Murty, K. L. (**1989**). "Applications of crystallographic textures of zirconium alloys in the nuclear industry," in *Zirconium in the nuclear industry: Eighth Int. Symp.*, American Society for testing and Materials, Philadelphia, pp. 570–595.

Santisteban, J. R., Vicente-Alvarez, M. A., Vizcaino, P., Banchik, A. D., Vogel, S. C., Tremsin, A. S., Vallerga, J. V., McPhate, J. B., Lehmann, E., and Kockelmann, W. (**2012**). "Texture imaging of zirconium based components by total neutron cross-section experiments," J. Nucl. Mater. **425**, 218–227.

Tenckhoff, E. (**2005**). "Review of deformation mechanism," J. ASTM Int. **2**, 25–50.

Vetvicka, I (**2014**). "Effect of creep and α-Zr ↔ (α + β)-Zr transition in Zr1Nb cladding on texture analyzed by neutron diffraction," J. Nucl. Mater. **453**, 196–201.

https://doi.org/10.1017/S0885715614001316 Published online by Cambridge University Press